A New Approach to Microclimate Analysis Using Airborne Remote Sensing, 3D-GIS and CFD Simulation

T.Asawa[1,*], A.Hoyano[2], T.Yoshida[3] and M.Takata[1]

[1]Interdisciplinary Graduate School of Science and Engineering, Tokyo Institute of Technology, Yokohama 2268502, Japan
[2]The Open University of Japan, Chiba 2618586, Japan
[3] PASCO Corporation, Tokyo 1530043, Japan

ABSTRACT

In order to make use of local, natural and climatic factors for urban development and passive building design, an understanding of microclimate in the locations of interest is required. The purpose of the present study is to show the characteristics of microclimates formed in a small city of paddy field areas using airborne remote sensing data, three-dimensional Geographic Information System (3D-GIS), and Computational Fluid Dynamics (CFD). The proposed method for analyzing microclimate combines airborne Multi-Spectral Scanner (MSS) data and a CFD simulation based on a 3D-GIS urban district model. The first step is to identify the actual land cover conditions in selected urban and surrounding areas of Tonami city using the airborne MSS data, GIS data, and aerial photographs. MSS data observed at noon and nighttime in spring, summer, and winter are used for the analysis. Land cover distribution maps and thermal images are generated from these data, and a 3D-GIS urban district model for the CFD simulation is completed. In the second step, these data are applied to the boundary conditions of a 3D, steady, CFD simulation, and air current and air temperature distributions in the area are simulated for three seasons, taking into account seasonal changes in land cover. The relationship between the land cover and surface temperature distributions of the Tonami urbanized area is examined based on the thermal images and land cover maps. The simulation results for the summer daytime show that cold air currents from the paddy fields flow into the urbanized area along a street, contributing to the decrease in air temperature in the area. The simulation results are compared with observation data along the street, and the accuracy of the simulation is confirmed. It is revealed that the control of air temperature by the paddy fields changes seasonally as its land cover changes through the year.

[*] Corresponding author email: asawa.t.aa@m.titech.ac.jp

KEYWORDS
Microclimate, Remote sensing, CFD, Air temperature, Land cover

INTRODUCTION

Changes in land cover distribution are a primary factor influencing the heat island effect in urbanized areas. The heat island effect has been observed not only in large cities, but also in smaller cities in the Japanese countryside. As urbanization progresses in a small city, housing development sprawls to the rural surroundings, and then the land cover changes from natural surfaces and vegetation to artificial materials, including asphalt pavements and reinforced concrete buildings with high heat capacities. In order to establish countermeasures against the heat island effect, it is necessary to understand the characteristics of land cover and local microclimates formed in these locations and their surroundings.

Tonami, a small city in Japan, is located in the Tonami plains, where widespread paddy fields cover most of the land surface. The Tonami urbanized area is surrounded by these paddy fields, so that their cooling effect could be utilized to mitigate the heat island effect in summertime (Yokohari 1998). Besides, there are regular seasonal changes in land cover on the paddy fields. The land cover of croplands in the study site, which is water in springtime due to irrigation, becomes green due to the growth of rice plants during summertime. In addition, these areas are covered with snow in wintertime. Therefore, the annual land cover change should be examined.

In a previous study, the authors' group implemented the analysis of nocturnal cold-air currents formed in urban neighboring hills and forests using airborne remote sensing data and a CFD simulation (Hoyano et al. 2007). The present study also applies this analysis method. The purpose of the present study is to clarify the relationship between the annual land cover change of the paddy fields and the seasonal characteristics of microclimate formed in the Tonami urbanized areas using airborne remote sensing data and a CFD simulation.

RESEARCH METHODS

Analysis steps

Firstly, we developed a method of analyzing the microclimate using a surface temperature distribution derived from the airborne multi-spectral scanner (MSS) data as a thermal boundary condition for the CFD simulation. In this process, the surface temperature data were overlaid on the 3D-GIS data of the region, and then the 3D surface temperature images were completed. Secondly, the land cover and surface temperature distributions were analyzed using the 3D surface temperature images for each season. Finally, the effects of the land cover of the paddy fields on the microclimate were examined using the CFD simulation results and field measurement results.

Airborne MSS

Observation by airborne MSS was performed in order to generate the land cover maps and surface temperature images of the Tonami plains, Japan, for May and July of

2002 and the winter of 2006, in both daytime and nighttime (Murakami 2007). Two observation altitudes were set: course 1 for high altitude was at 6,000 m, which allowed observation of the entire Tonami plains, and course 2 for low altitude was at 1,500 m, which allowed observation of detailed ground surface information. Spatial resolutions on the ground were 8.0 m and 2.0 m, respectively. Figure 1 shows the observation courses. Table 1 lists the observation date and time for each season and Table 2 gives the specifications of the MSS data.

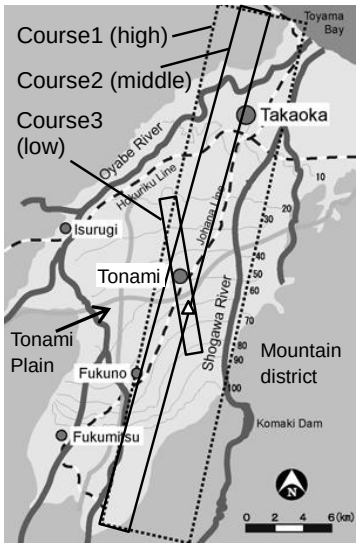

Figure 1. *Observation course of the airborne MSS*

Table 1. *Observation date and time for each season*

	Spring daytime	Spring nighttime	Summer daytime	Summer nighttime	Winter daytime	Winter nighttime
Date	2002/5/25	2002/5/21	2002/7/25	2002/7/26	2006/2/22	2006/2/21
Couse1	11:30-11:45	20:28-20:40	12:00-12:12	20:07-20:20	12:29-12:49	19:02-19:15
Course2	12:09-12:24	19:43-19:54	12:33-12:42	19:19-19:30	13:34-13:48	18:28-18:40

Table 2. *Specification of the MSS data*

Spring and Summer		Winter	
Band	Wave length(nm)	Band	Wave length(nm)
1	459～489	1	459～489
2	542～564	2	551～579
3	586～614	3	586～614
4	655～679	4	655～679
5	683～713	5	825～871
6	738～768	6	976～1114
7	825～871	7	1026～1166
8	976～1114	8	1229～1375
9	1430～1570	9	1430～1570
10	1582～1666	10	1583～1695
11	6675～11815	11	6675～11815
12	10105～13525	12	10105～13525

Generation of land cover maps

In advance of the land cover distribution analysis, we conducted a rectification and land cover classification using the airborne MSS and GIS data. First, rectification was performed by a second-order polynomial transformation using the airborne MSS data and GIS data drawn on a scale of 1:5000. Extracting a small area from the rectified MSS data, six polygon items were created as a signature, and supervised classification was implemented. By considering the land cover change, the land cover maps including vegetative areas were generated.

Generation of the 3D urban district model

The 3D urban district model was made by combining GIS data with the land cover maps (2.0 m resolution) generated from the MSS data (Figure 2). The building models were made by adding building height information (multiplying stories by floor height) onto the building 2D polygon of the GIS data. Two types of buildings were used, one with a wooden structure and the other made of reinforced concrete. The tree models were generated by combining tree height information with the tree distribution derived from the land cover maps. The tree model considered three distinct tree heights, obtained from field measurements in this region. The building and tree models were added to the land cover maps to complete the 3D urban district model.

Generation of the 3D surface temperature image

Surface temperature images, generated from the MSS data, were applied to the building roofs and ground of the 3D urban district model. The surface temperatures of building walls cannot be obtained from the MSS data, so the wall temperatures were calculated by a 3D CAD-based thermal environment simulator, which was developed by the authors' group (Asawa 2008). The temperature of the tree crowns was determined by the vegetative (tree) coverage area of the surface temperature images. These processes allowed us to complete the 3D surface temperature images for each season (Figure 2).

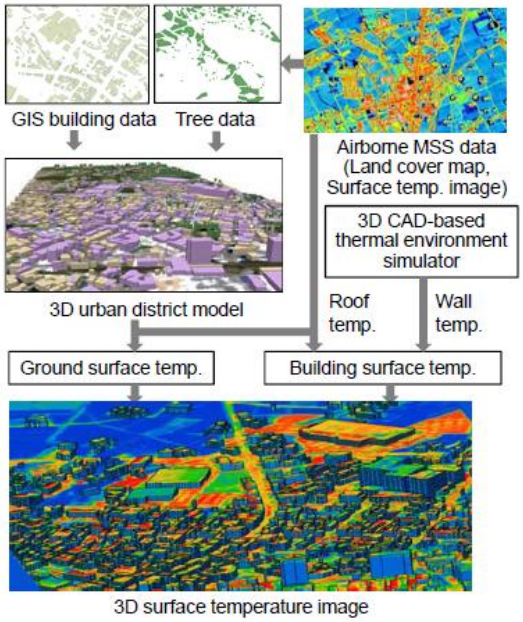

Figure 2. *Generation of the 3D urban district model and 3D surface temperature image*

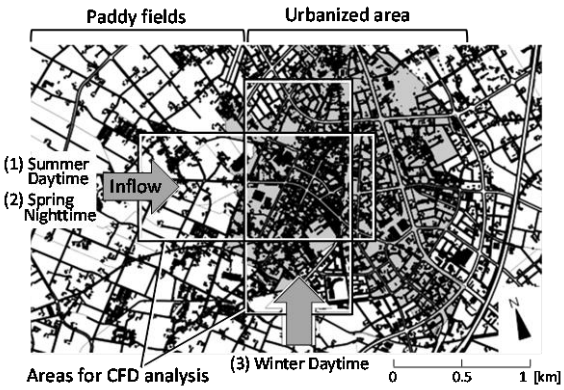

Figure 3. *Subject area for the microclimate analysis using CFD simulation (including the field measurement points)*

CFD simulation

The subject area for the microclimate analysis using a CFD simulation includes the Tonami urbanized area and its surrounding paddy fields. This subject area includes the positions used for the microclimate field measurements conducted in the summertime, so that these data can be compared with each other (Figure 3).

The 3D surface temperature images generated in the previous step were used for the thermal boundary conditions (input data) for the CFD simulation, and then the airflow and air temperature distribution in the subject area were calculated. Three-dimensional turbulent airflow was given by Reynolds-averaged Navier–Stokes equations (RANS). The governing flow equations were solved with the SIMPLE algorithm. A numerical scheme (QUICK) was used for the pressure correction in solving the governing equations. The standard k–ε model was used for the turbulence model and the Boussinesq approximation was used for the buoyancy-driven flow. Table 3 shows the details of the CFD simulation. Figure 4 illustrates the 3D model for the CFD simulation.

Inflow air temperature and velocity were set using the AMeDAS (Automated Meteorological Data Acquisition System) data at Tonami city, where the weather station is located in the paddy field area. The CFD simulation was conducted for three seasons.

Table 3. *Details of CFD simulation*

Dimension	2050m(X) x 895m(Y) x 100m(Z)
Grid number	1513 (X) x 895 (Y) x 43 (Z)
Minimum grid size	1m (for X and Y), 0.5m (for Z)
Turbulence model	Standard K-ε model
Solid surface	Log law for smooth surface Convective heat transfer coefficient 11.6W/m^{2}K
Top and sides of simulation domain	Free-slip
Inflow boundary	Power law (power index 0.15) Wind velocity and temperature at the standard position are derived from Tonami AMeDAS data.
Outflow boundary	Free
Inflow wind direction	(1) Daytime in the summer: ENE (2) Nighttime in the spring: ENE (3) Daytime in the summer: SSW

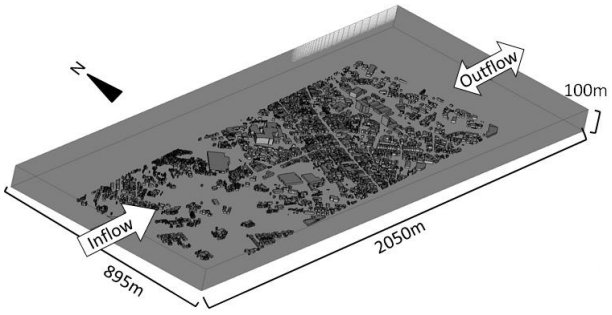

Figure 4. *3D model for CFD simulation (wind direction is for the case of daytime in the summer and nighttime in the spring)*

RESULTS AND DISCUSSION

Comparison between the simulation result and observation result

Figure 5 shows a comparison between the CFD simulation result and field measurements of air temperature and wind velocity distribution along a wide street in the summertime. The field measurements were conducted along the street from the paddy fields to the urbanized area in the summer of 2004. The position for measuring air temperature and wind velocity was set at a height of 1.5 m.

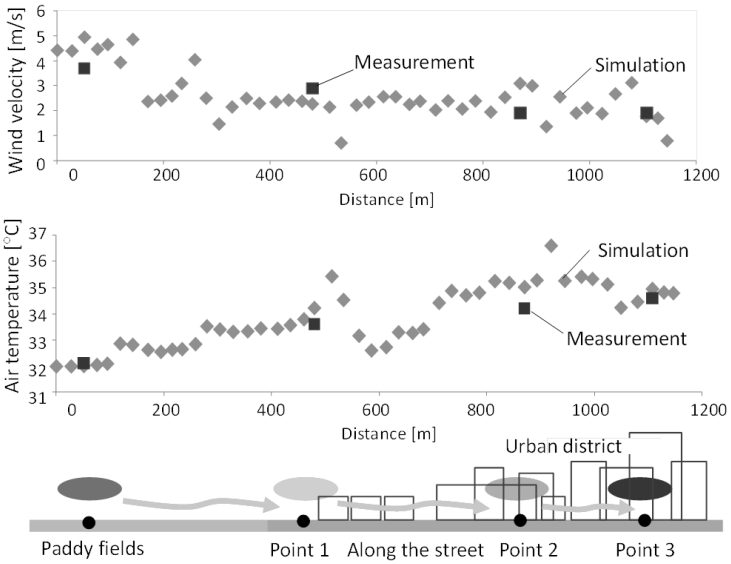

Figure 5. *Comparison between simulation and observation (summer, daytime)*

The simulation result indicates that the wind velocity decreases gradually from the open paddy fields into the urbanized area. The difference in wind velocity between the inside and outside of the urbanized area is approximately 2 m/s. The air temperature simulation indicates that air currents with a lower temperature (cool air current) flow from the paddy field along the street, reaching approximately 400 m inside the edge of the urbanized area.

The observation results for wind velocity and air temperature show the same distribution as the simulation results. Therefore, this confirms that the CFD simulation results are appropriate for discussion.

Simulation results for each season

A CFD simulation was conducted for three cases to account for the characteristics of land cover and surface temperature distributions: (1) Daytime in summer, (2) Nighttime in spring, (3) Daytime in winter.

Figure 6 shows the 3D surface temperature images and the CFD simulation results of the wind velocity and air temperature distribution for each case.

(1) Daytime in summer

The land cover of the paddy fields around the urbanized area is green due to the growth of rice plants. The surface temperature distribution image indicates that the surface temperature of the paddy fields is much lower than the air temperature, and approximately 30°C lower than the asphalt paved ground in the urbanized area. The simulation of air temperature distribution shows that the air temperature in the central urbanized area is much higher than that in the windward paddy fields, confirming the occurrence of a heat island effect.

The cool air current from the windward paddy fields flows into the urbanized area along the wide street, decreasing the air temperature in the urbanized area. However, the cool air current does not go beyond the crossroads at the center of the urbanized area. The air temperature increases to the leeward of the buildings and narrow streets, where the air current stagnates and the surface temperature of the space increases.

(2) Nighttime in spring

Due to irrigation, the land cover of the paddy fields is water in springtime, so the urbanized area is surrounded by water fields. The average surface temperature of the paddy fields is approximately 18°C, only 3°C lower than that of the asphalt pavement in the urbanized area. This is due to the high heat capacity of water and its solar heat storage during the daytime. The difference in air temperature between the paddy fields and urbanized area is also small.

(3) Daytime in winter

In winter, the main wind direction over this region is southwesterly. The wind velocity in the paddy fields is approximately 3 m/s. The air current flowing into the urbanized area is blocked by the windward buildings and windbreak forests situated on the southern edge of the area, causing the wind velocity in most of the urbanized area to remain below 1.5 m/s.

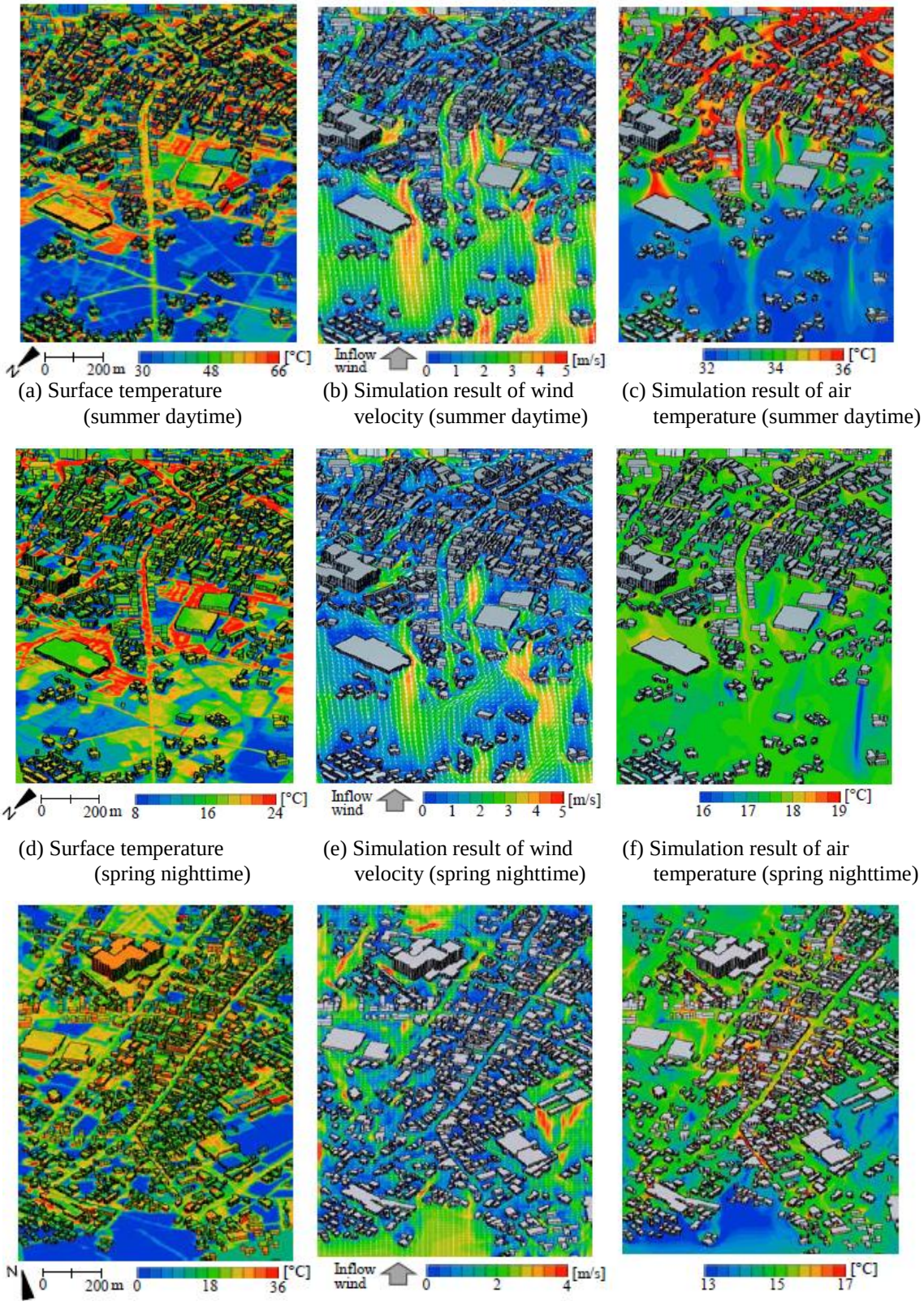

(a) Surface temperature (summer daytime)

(b) Simulation result of wind velocity (summer daytime)

(c) Simulation result of air temperature (summer daytime)

(d) Surface temperature (spring nighttime)

(e) Simulation result of wind velocity (spring nighttime)

(f) Simulation result of air temperature (spring nighttime)

(g) Surface temperature (winter daytime)

(h) Simulation result of wind velocity (winter daytime)

(i) Simulation result of air temperature (winter daytime)

Figure 6. *3D surface temperature images, CFD simulation results of wind velocity and air temperature distribution for each case*

The land cover of the paddy fields is snow, and the surface temperature is approximately 20°C lower than that in the urbanized area. The difference in air temperature between the paddy fields and the urbanized area is 2°C; the heat island effect is confirmed in this season as well as in the summer. Solar altitude is lower than in the summer, so the southern walls of buildings receive large amounts of solar radiation and their surface temperature increases. The air temperature around the buildings, therefore, increases. This is characteristic of the microclimate formed in this season.

These results indicate that the control of microclimate by the paddy fields changes seasonally as its land cover changes through the year.

CONCLUSIONS

This paper presented a method for analyzing microclimate in a small town of paddy field areas using airborne MSS data and a CFD simulation. The 3D urban district model and 3D surface temperature image were generated by combining MSS data and GIS data for Tonami city. The relationship between the land cover of the paddy fields and the microclimate formed inside and outside the Tonami urbanized area were analyzed using the 3D surface temperature image and CFD simulation for three seasons, taking into account the seasonal land cover change.

These results quantitatively indicated that the control of microclimate by the paddy fields changes seasonally as its land cover changes through the year. In the summertime, the cooling effect of the paddy fields and the cool air currents from the area contributed to the decrease in air temperatures in the urbanized area. In the spring, the nighttime difference in both surface and air temperature between the paddy fields and urbanized area was small, due to the high heat capacity of irrigated water on the paddy fields. In the winter, the air temperature in the urbanized area was much higher than that in the snow-covered paddy fields, so that the heat island effect was confirmed.

REFERENCES

Asawa T. Hoyano A. and Nakaohkubo K. 2008. Thermal design tool for outdoor spaces based on heat balance simulation using a 3D-CAD system, *Building and Environment*. 43, pp. 2112-2123.

Hoyano A. He J. and Kita H. 2007. Analysis of formation of nocturnal cold-air currents in satoyama using airborne MSS data and CFD, *J. of The Remote Sensing Society of Japan*. 27(5), pp.445-455. (In Japanese with English Abstract)

Murakami A. Hoyano A. and Kim K. 2007. Relationship between the land cover change and the thermal environment in an agricultural region of Japan using multi-temporal airborne MSS, *Proc. of IGARSS 2007*. pp. 1786-1789.

Yokohari M. 1998. Effect of paddy fields on summertime air temperature in urban fringe areas; a case study in Kasukabe city, Saitama prefecture, *J. Jap. Inst. Landscape Architect*. 61(5), pp.731-736. (In Japanese with English Abstract)